Synthesis, Spectroscopic, NLO And Molecular Docking Analysis Of (2E)-3-(1H-Indol-2-yl)-N-Phenylprop-2-Enamide

S. Abbas Manthiri[1], R. Raj Muhamed[2], V. Sathyanarayanamoorthi[3], M. Raja[4], S. Arulappan[5]

[1, 2, 3, 4, 5] Dept of Physics

[1, 2, 5] Jamal Mohamed College, Tiruchirappalli 620020, Tamil Nadu, India.

[3]PSG College of Arts and Science, Coimbatore 641014, Tamil Nadu, India.

[4]Govt Thirumagal Mills College, Gudiyattam 632602,Vellore, Tamil Nadu, India.

Abstract- *The title compound, (2E)-3-(1H-indol-2-yl)-N-phenylprop-2-enamide (2INP) has been synthesized and characterized by FT-IR and FT-Raman spectral analysis. The molecular structure, fundamental vibrational frequencies and intensity of the vibrational bands are interpreted with the aid of the structure optimizations and normal coordinate force field calculations based on density functional theory (DFT) method using 6-311++G(d,p) basis set. A complete assignment and analysis of the fundamental vibrational modes of the molecule were carried out. The vibrational studies were interpreted in terms of potential energy distribution. Besides NLO were also calculated and interpreted. To study the biological activity of the investigation molecule, molecular docking was done to identify the hydrogen bond lengths and binding energy with different antimicrobial protein.*

Keywords- DFT; FT-IR; FT-Raman; NLO; Molecular docking

I. INTRODUCTION

The synthesis of enamide and indol derivatives has generated vast interest to organics as well as for medicinal chemistry, agricultural and many other industrial processes [1]. Several enamide and indol derivatives have proved the efficiency and efficacy in combating various diseases. Particularly, enamide and indol derivatives of (2E)-3-(1H-indol-2-yl)-N-phenylprop-2-enamide (2INP) wide variety of biological activities such as antifungal, antibacterial, antituberculosis, antitumor, hypoglycemic, anti-inflammatory, analgesic and antipyretic activities [2-3]. Its chemical formula is C17H14N2O.

To our knowledge, Literature survey reveals that the DFT/B3LYP frequency calculations of (2E)-3-(1H-indol-2-yl)-N-phenylprop-2-enamide (2INP) have not been carried out so far. In this present work, we report the synthesis and comprehensive spectroscopic investigation of 2INP using B3LYP/6-311++G(d,p) level of the theory. The experimental spectral data (FT-TR, and FT-Raman) of the 2INP is compared by means of the theoretical spectral data obtain by DFT/B3LYP method 6-311++G(d,p) basis set.

II. MATERIAL AND METHODS

Synthesis

A mixture of 1.35g N-phenylacetamide (0.01 mol) and 1.45g 1H-indole-2-carbaldehyde (0.01 mol) was stirred in ethanol (30ml). To this aqueos solution of NaOH added to it after 30 minutes and continuous stirring for 4 hrs. The mixture was kept overnight at room temperature and then it was poured into crushed ice and acidified with HCl. The solid separated was filtered and crystallized from ethanol. The reaction scheme is shown in Fig.1.

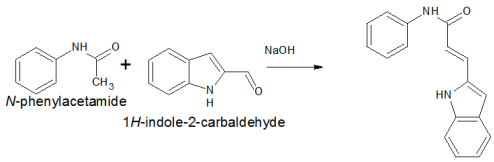

Fig. 1. The scheme of the synthesis of 2INP

Experimental

The FT-IR spectrum of the synthesis compound (2E)-3-(1H-indol-2-yl)-N-phenylprop-2-enamide (2INP) was recorded in the region 4000-450 cm-1 in evacuation mode using a KBr pellet technique with 1.0 cm-1 resolution on a PERKIN ELMER FT-IR spectrophotometer. The FT-Raman spectrum of the 2INP compound was recorded in the region 4000-100 cm-1 in a pure mode using Nd: YAG Laser of 100 mW with 2 cm-1 resolution on a BRUCKER RFS 27 at SAIF, IIT, Chennai, India.

Computational details

The entire calculations (vibrational wavenumbers, geometric parameters, and other molecular properties) were

implemented by using GaussView 5.0 program [4] and Gaussian 09W program package on a computing system [5]. The molecular structure of 2INP the ground state (in the gas phase) was optimized by DFT/B3LYP methods with 6-311++G(d,p) basis set level, and the optimized structure was used in the vibrational frequency calculations.

III. RESULTS AND DISCUSSION

Molecular geometry

The molecular structure along with numbering of atoms of 2INP is obtained from Gaussian 09W and GaussView 5.0 programs are shown in Fig.2. The bond parameters (bond length and bond angles) of the 2INP molecules are listed in Table 1 using DFT/B3LYP method with 6- 311++G(d,p) basis set. To the best of our knowledge, exact experimental data on the geometrical parameters of 2INP are not available in the literature. Therefore, the crystal data of a closely related molecule such as (E)-2-Cyano-3-[4-(dimethylamino)-phenyl]-N-phenylprop-2-enamide [6] is compared with that of the title compound. The theoretical calculations were carried out isolated molecule in the gaseous phase the experimental results are for a molecule in a solid state.

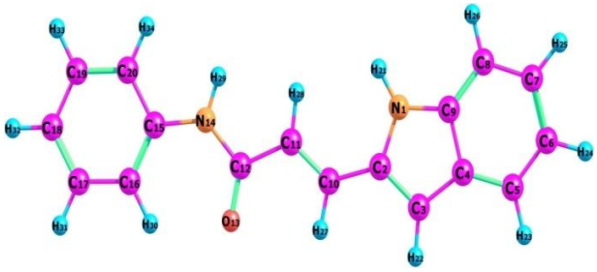

Fig. 2. Optimized geometric structure with atoms numbering of 2INP

This title molecule has sixteen C - C bond lengths, thirteen C - H bond lengths, three (N-C), two N - H bond lengths and one (C – O, C-N) bond lengths respectively. The highest bond length was calculated for C11 – C12, N14 – C15 found to be 1.492 and 1.445 Å. The calculated bond length values for C-C and C-H in the benzene ring vary from 1.484-1.347 Å and 1.404-1.079 Å by B3LYP/6-311G(d,p) basis set. The C-C bond lengths are higher than the C-H bond lengths.

Vibrational analysis

Vibrational spectroscopy is used extensively in organic chemistry for the identification of functional groups of organic compounds, the study of molecular confirmations, kinetics, reaction etc. The complete vibrational assignments of fundamental modes of 2INP along with the PED are given in Table 2. The title molecule consists of 34 atoms, which has 96 normal modes of vibration. Potential energy distribution (PED) was computed for each normal mode among the symmetry coordinates of the molecule. Based on the computed PED values and FT-IR intensities and FT-Raman band activities a detailed assignment of the fundamentals was proposed. The calculated wavenumbers are scaled using the scaling factor 0.961. The comparative observed and simulated FT-IR and FT-Raman spectra are shown in Fig 3. The calculated vibrational frequencies (Unscaled and Scaled), IR intensity, Raman activity are tabulated in Table 2.

C-H vibrations

In the aromatic compounds, the C-H stretching wavenumbers appear in the range 3000-3100 cm^{-1} which are the characteristic region for the ready identification of C-H stretching vibrations [7]. The C-H stretching and bending regions are of the most difficult regions to interpret in infrared spectra. The nature and position of the substituent cannot affect these vibrations. Most of the aromatic compounds have almost four infrared peaks in the region 3080-3010 cm-1 due to ring C-H stretching bands [8]. In this present study, the C-H stretching vibrations are observed at 3117, 3113, 3067, 3047, 3044, 3024 and 3014 cm-1 by B3LYP/6-311++G(d,P) method show good agreements with experimental vibrations. The bands observed in the recorded FT-IR spectrum 3105(vs), 3044(s), 2977(s) cm-1 and with the FT-Raman spectrum bands at 3115(m), 3103(m), 3078(s), 3064(s) , 3064cm-1. The PED corresponding to this pure mode of title molecule contributed 99, 99, 92, 95, 95, 99, 90 and 98% is shown in Table 2.

C-C ring vibrations

The C-C stretching vibrations are expected in the range from 1650 to 1100 cm-1 which are not significantly influenced by the nature of the substituents [9]. The C-C stretching vibrations of the 2INP compound were observed from1600 to 810 cm^{-1}

Table 1 Optimized geometrical parameters of (2E)-3-(1H-indol-2-yl)-N-phenylprop-2-enamide (2INP) obtain by B3LYP/6-311++G(d,p) basis set

Parameters	Expa	B3LYP	Parameters	Expa	B3LYP
Bond length(Å)			Bond angle(o)		
N1-C2	1.422	1.391	C2-C10-C11	125.7	127.8
N1-C9	1.359	1.377	C2-C10-H27	114.0	115.6
N1-H21	0.860	1.006	C4-C3-H22	120.0	127.2
C2-C3	1.385	1.383	C3-C4-C5	131.6	134.3
C2-C10	1.424	1.436	C3-C4-C9	116.1	106.7
C3-C4	1.424	1.427	C5-C4-C9	119.4	119.0
C3-H22	0.960	1.079	C4-C5-C6	119.4	119.0
C4-C5	1.407	1.407	C4-C5-H23	120.0	120.4
C4-C9	1.424	1.423	C4-C9-C8	122.4	122.1
C5-C6	1.385	1.385	C6-C5-H23	120.0	120.7
C5-H23	0.960	1.084	C5-C6-C7	121.3	121.1
C6-C7	1.407	1.411	C5-C6-H24	120.0	119.8
C6-H24	0.960	1.084	C7-C6-H24	119.0	119.2
C7-C8	1.390	1.388	C6-C7-C8	121.3	121.4
C7-H25	0.960	1.084	C6-C7-H25	119.0	119.3
C8-C9	1.397	1.397	C8-C7-H25	119.0	119.3
C8-H26	0.960	1.084	C7-C8-C9	117.7	117.5
C10-C11	1.347	1.347	C7-C8-H26	120.0	121.1
C10-H27	0.960	1.086	C9-C8-H26	120.0	121.5
C11-C12	1.492	1.484	C11-C10-H27	114.0	116.6
C11-H28	0.960	1.087	C10-C11--C12	119.9	120.0
C12-O13	1.216	1.223	C10-C11-H28	120.0	121.8
C12-N14	-	1.383	C12-C11-H28	119.0	118.2
N14-C15	1.445	1.409	C11-C12-O13	-	123.1
N14-H29	0.860	1.009	C11-C12-N14	-	113.3
C15-C16	1.407	1.402	O13-C12-N14	124.0	123.6
C15-H20	0.960	1.404	C12-N14-C15	128.4	129.4
C16-C17	1.393	1.394	C12-N14-H29	116.0	115.9
C16-H30	0.960	1.079	C15-N14-H29	116.0	114.7
C17-C18	1.393	1.393	N14-C15-C16	124.7	123.5
C17-H31	0.960	1.084	N14-C15-C20	116.3	117.2
C18-C19	1.397	1.395	C16-C15-C20	119.4	119.3
C18-H32	0.960	1.084	C15-C16-C17	119.4	119.3
C19-C20	1.390	1.389	C15-C16-H30	120.0	119.5
C19-H33	0.960	1.084	C15-C20-C19	120.5	120.6
C20-H34	0.960	1.086	C15-C20-H34	120.0	119.7
Bond angle(o)			C17-C16-H30	120.0	121.1
C2-N1-C9	116.3	109.7	C16-C17-C18	121.3	121.4
C2-N1-H21	116.0	125.2	C16-C17-H31	119.0	118.7
N1-C2-C3	114.8	108.2	C18-C17-H31	120.0	119.9
N1-C2-C10	124.7	124.4	C17-C18-C19	119.0	119.1
C9-N1-H21	116.0	125.1	C17-C18-H32	120.0	120.5
N1-C9-C4	114.8	107.4	C19-C18-H32	120.0	120.4
N1-C9-C8	124.7	130.5	C18-C19-C20	120.5	120.2
C3-C2-C10	125.7	127.5	C18-C19-H33	120.0	120.3
C2-C3-C4	116.1	107.9	C20-C19-H33	120.0	119.5
C2-C3-H22	120.0	124.8	C19-C20-H34	120.0	119.7

[a] Taken from Ref [6]

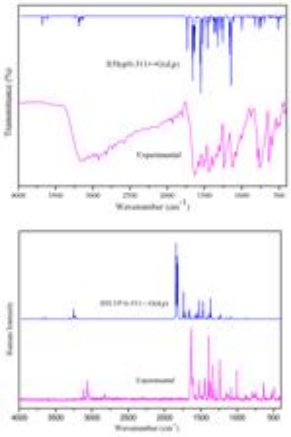

Fig. 3. FT- IR and FT-Raman spectra of 2INP (Experimental, B3LYP/6-311++G(d,p))

In this present study, the C-C stretching vibrations are found at 1574(vs), 1519(vs), 1496(vs), 1422(vs), 1334(s), , 1295(s), 1081(s), 1004(m) cm^{-1} in FT-IR and 1615(s), 1575(m), 1521(s), 1498(s), 1485(s), 1477(m), 1394(vs), 1336(vs), 1150(m), 1085(vs), 1007(s), 995(vw), 964(vw), 959(w), 827(m) 810(vw) cm^{-1} in FT-Raman respectively. The theoretical wavenumbers at 1598, 1576, 1522, 1499, 1472, 1468, 1465, 1407, 1382, 1274, 1155, 1095, 1009, 993, 965, 961, 825 and 813 cm-1 are assigned as C-C stretching vibrations with PED contribution of 66, 59, 67, 34, 26, 47, 16, 14, 64, 36, 20, 18, 63, 66, 43, 22, 53 and 40% respectively.

Hyperpolarizability calculation

Non-linear optical (NLO) property is the forefront of present research because of its significance in grants the key functions of frequency shifting, optical modulation, optical switching, optical logic, and optical memory for the emerging technologies in areas such as telecommunications, signal processing, and optical interconnections [10,11]. Urea is the prototypical molecule utilized in investigating of the NLO properties of the compound. For this reason, urea was used often as a threshold value for comparative purpose. The calculated dipole moment and hyperpolarizability values obtained from B3LYP/6-311++G(d,p) methods are collected in Table 3. The first order hyperpolarizability of 2INP with B3LYP/6-311++G(d,p) basis set is 2.6366×10^{-30} two times greater than the value of urea ($\beta o = 0.6230$ x 10-30 esu). From the computation, the high values of the hyperpolarizabilities of 2INP are probably attributed to the charge transfer existing amid the benzene rings within the molecular skeleton. This is evidence for the nonlinear optical (NLO) property of the molecule.

Table 2 Calculated vibrational frequencies (cm^{-1}) assignments of 2INP based on B3LYP/6-311++G(d,p) basis set.

Mode no	Experimental wave number (cm^{-1})		Theoretical wave number(cm^{-1})		I_{IR} [c]	I_{RAMAN} [d]	Assignments (PED)[a,b]
	FTIR	FT-Raman	Unscaled	scaled			
96		-	3677	3533	13	1	γNH(100)
95	3445(w)	-	3617	3476	5	3	γNH(100)
94		3115(s)	3243	3117	2	1	γCH(99)
93	3105(vs)	3103(m)	3239	3113	0	1	γCH(99)
92		3078(s)	3192	3067	4	9	γCH(92)
91		3064(s)	3191	3067	10	5	γCH(95)
90		-	3181	3057	7	2	γCH(97)
89		-	3177	3053	6	2	γCH(91)
88		3046(s)	3171	3047	0	3	γCH(95)
87	3044(s)	-	3168	3044	0	0	γCH(99)
86		-	3168	3044	0	2	γCH(89)
85		-	3164	3041	0	0	γCH(97)
84		3029(s)	3147	3024	4	1	γCH(90)
83	2977(s)	-	3137	3014	5	1	γCH(98)
82	1633(vs)	1631(vs)	1735	1667	47	0	γOC(71)
81		1615(s)	1663	1598	85	100	γCC(66)
80		-	1651	1586	42	80	γCC(62)
79	1574(vs)	1575(m)	1640	1576	47	71	γCC(59)+βHCC(19)
78		-	1632	1569	18	0	γCC(60)+βHCC(12)
77	1519(vs)	1521(s)	1615	1552	1	1	γCC(67)
76	1496(vs)	1498(s)	1560	1499	58	1	γCC(34)+βHNC(17)
75		1485(s)	1552	1492	100	36	γCC(26)+βHNC(42)
74		1477(m)	1527	1468	0	0	γCC(47)+βHCC(22)
73	1442(vs)	1460(s)	1524	1465	38	9	βHCC(52)+γNC(-13)+γCC(16)
72		-	1472	1415	7	9	γCC(24)+βHNC(13)
71		1394(vs)	1464	1407	44	13	βHCC(51)+γCC(14)
70	1389(vs)	1373(s)	1438	1382	9	2	βHNC(29)+γNC(16)
69	1334(s)	1336(vs)	1389	1335	6	1	γCC(64)+γ
68		-	1371	1317	22	6	βHCC(58)+γCC(13)
67		-	1356	1303	15	6	γCC(41)+βHCC(32)
66		1298(m)	1355	1302	8	2	βHCC(69)
65	1295(s)	-	1326	1274	41	3	γCC(36)+βHCC(22)
64		-	1320	1268	0	26	γNC(53)
63	1241(vs)	1243(vs)	1289	1238	18	2	βHCC(57)
62		-	1260	1211	35	24	βHCC(10)+γNC(51)
61		-	1253	1204	16	9	βHCC(43)
60		-	1243	1194	4	0	βCCC(10)+βHCC(22)+γNC(28)
59		1150(m)	1202	1155	1	3	γCC(20)+βHCC(72)
58		-	1183	1137	2	1	βHCC(-72)
57		-	1179	1133	0	0	βHCC(-66)+γCC(10)
56	1124(vs)	1126(s)	1166	1121	50	7	γNC(34)+βHCC(11)
55		-	1150	1105	93	28	γNC(14)+βHCC(46)
54	1081(s)	1085(vs)	1139	1095	4	3	γCC(18)+βHCC(46)

53		-	1111	1068	8	1	βHCC(21)+γCC(49)
52	1004(m)	1007(s)	1050	1009	0	0	γCC(63)+βHCC(23)
51		995(w)	1033	993	1	3	γCC(66)
50		971(vw)	1014	975	1	0	βCCC(63)
49		964(vw)	1004	965	2	2	γCC(43)+βHNC(23)
48		-	1002	963	1	0	τHCCN(-91)
47		-	1000	961	9	5	τHCCC(63)+τHCCC(-18)
46		959(w)	1000	961	9	1	γCC(22)
45		950(w)	978	940	0	0	τHCCH(89)
44		933(vw)	976	938	0	0	τHCCN(94)
43		907(w)	942	905	1	0	τHCCH(85)
42	883(w)	884(m)	915	879	2	0	τHCCH(94)
41		871(s)	907	871	1	2	βCCC(66)
40		827(m)	859	825	1	0	γCC(53)
39		-	857	824	0	0	τHCCC(79)
38		-	849	816	3	0	τHCCC(79)
37		810(vw)	846	813	0	3	γCC(40)+βCCC(12)
36		-	839	806	0	0	τHCCN(92)
35	787(s)	789(m)	820	788	15	0	τHCCC(80)
34	760(vs)	764(m)	796	765	1	0	βHCC(45)+γCC(12)
33		742(s)	767	737	17	0	τHNCC(87)
32		722(m)	764	734	4	0	τHCCC(87)
31		715(vw)	748	719	15	0	τHCCC(86)
30		701(w)	731	702	1	0	τCNCO(80)
29		671(w)	703	676	10	0	τHCCC(94)
28		-	697	670	1	0	γCC(11)+βCCC(24)+βHNC(22)
27	638(vs)	-	641	616	1	0	OUTCCNC(76)
26		607(m)	633	608	1	0	βHCC(83)
25	598(m)		618	594	3	1	βCCC(61)
24		581(w)	600	577	2	0	βCCO(74)
23		559(w)	576	554	0	0	τHCCC(89)
22	529(m)	530(m)	552	530	3	0	βCCC(56)
21		-	519	499	12	0	τHNCC(78)
20	492(m)	493(s)	517	497	10	0	τHCCC(87)
19	450(w)	462(w)	491	472	6	0	βCCC(56)
18	426(w)	431(w)	449	431	2	0	τHCCC(81)
17	-	411(m)	417	400	0	0	τHCCC(96)
16	-	381(w)	383	368	1	0	βNCO(67)
15	-	363(m)	375	360	3	0	τHNCC(56)
14	-	335(w)	349	336	0	0	βCNC(71)
13	-	-	327	314	10	0	τHCCN(23)+τHNCC(24)
12	-	-	262	251	0	0	τCCCN(58)
11	-	-	251	241	3	0	βCCC(83)
10	-	-	250	240	0	0	τCCCN(78)
9	-	188(m)	195	187	0	0	βHNC(14)+γCC(41)
8	-	169(s)	188	181	4	0	τHCCO(65)
7	-	145(m)	153	147	0	0	τHCCC(-39)+τHCCN(39)
6	-	104(vs)	126	121	0	0	βCCN(80)

5	-	-	68	66	1	0	τHNCC(55)
4	-	-	61	59	0	0	τCNCC(61)+τHCCC(10)
3	-	-	40	39	0	0	βCCC(91)
2	-	-	27	26	0	0	τCNCC(59)
1	-	-	24	23	0	0	τCCNC(71)

[a]γ-stretching,γ_a-Symmetrical stretching,γ_{as}-asymmetrical stretching, β- inplane bending ,ω- outplane bending, τ-torsion, vs-very strong, s- strong, m-medium, w-weak.
[b]scaling factor : 0.961 for B3LYP/6-311+G(d,p)
[c]Relative absorption intensities normalized with highest peak absorption equal to 100.
[d]Relative Raman intensities normalized to 100.

Table 3 The values of calculated dipole moment□□ (D), polarizability (□$_0$), first order hyperpolarizability (βtot) components of 2INP

Parameters	**B3LYP/6-311++G(d,p)**	**Parameters**	**B3LYP/6-311++G(d,p)**
□$_x$	0.4137	β_{xxx}	102.863
□$_y$	1.5693	β_{xxy}	-1.1978
□$_z$	-0.0001	β_{xyy}	184.0627
□(D)	1.6229	β_{yyy}	44.6044
□$_{xx}$	491.9038	β_{zxx}	-0.7517
□$_{xy}$	-5.4998	β_{xyz}	0.04131
□$_{yy}$	212.9656	β_{zyy}	0.0034
□$_{xz}$	0.0030	β_{xzz}	10.2785
□$_{yz}$	-0.0067	β_{yzz}	25.948
□$_{zz}$	113.0288	β_{zzz}	-0.0121
□□□**e.s.u**□	4.0404x10^{-23}		
Δ□□**e.s.u**□	13.5960 x10^{-23}	βtot (e.s.u)	2.6366X10^{-30}

Molecular docking study

AutoDock suite 4.2.6 is a recently been used as a convenient tool to get insights into the molecular mechanism of protein-ligand interactions, bind to a receptor of known three-dimensional structure. With the aim to investigate the binding mode, a molecular modeling study was performed using AutoDock Tools for docking [12]. 2INP was selected to be docked into the active site of three receptors 4HBU, 4HOE and 3EQA of antimicrobial proteins which was downloaded from RCSB protein data bank (http://www.rcsb.org/pdb/home/home.do) [13]. The ligand was docked into the functional sites of the respective proteins individually and the docking energy was examined to achieve a minimum value. AutoDock results indicate the binding position and bound conformation of the peptide, together with a rough estimate of its interaction. Docked conformation which had the lowest binding energy was chosen to investigate the mode of binding. The molecular docking binding energies (kcal/mol) and inhibition constants (μm) were also obtained and listed in Table 4. Among them, 4HOE exhibited the lowest free energy at −7.54 kcal/mol and most docked inhibitors interacted with the ligand within the 4HOE binding site. They exhibited up to two N H …O hydrogen bonds involving ALA 11and ILE 19 with RMSD being 27.78 Å. The docking simulation shows the binding mode of the 2INP into 4HOE. The 2INP ligand interacts with different receptors are shown in Figs. 4-6.

Table 4 Hydrogen bonding and molecular docking with antimicrobial protein targets

Protein (PDB ID)	Bonded residues	No. of hydrogen bond	Bond distance (Å)	Estimated Inhibition Constant (μm)	Binding energy (kcal/mol)	Reference RMSD (Å)
4HBU	TRP 229	1	2.3	35.68	-6.07	23.66
4HOE	ALA 11	2	2.3	2.97	-7.54	27.78
	ILE 19		1.9			
3EQA	ARG 329	3	1.7	41.62	-5.98	24.38
	GLU 203		2.3			
	GLU 203		2.0			

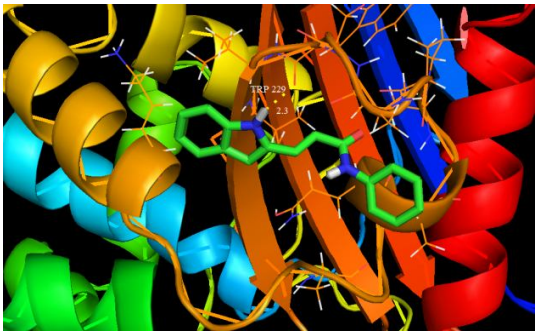

Fig. 4. Docking and Hydrogen bond interactions 2INP with chain A of 4BHU protein structure.

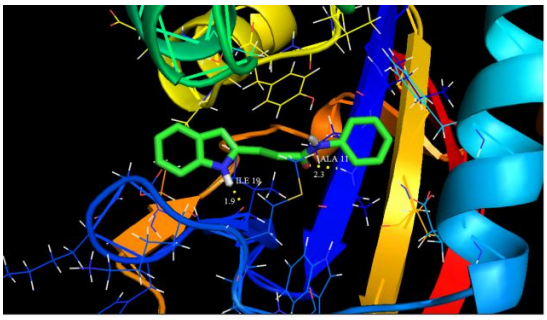

Fig. 5. Docking and Hydrogen bond interactions 2INP with chain A of 4HOE protein structure

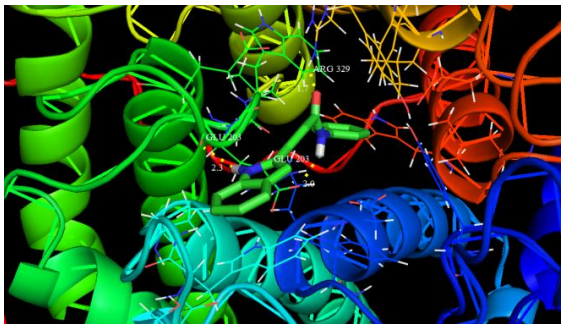

Fig. 6. Docking and Hydrogen bond interactions 2INP with chain A of 3EQA protein structure

IV. CONCLUSION

In the present work, we have reported on experimental and theoretical spectroscopic analysis of 2INP molecule using FT-IR, FT-Raman and tools derived from the DFT. In general, a good agreement amid experimental and theoretical normal modes of vibrations has been investigated. The molecular optimized geometry, vibrational frequencies, infrared intensities and Raman activity of the molecule have been calculated by using DFT/B3LYP method with 6-311++G(d,p) basis set. All the theoretical results show good correspondence with experimental data. The nonlinear optical properties are also addressed theoretically. The title compound may be a potential applicant in the development of NLO materials. Furthermore, the molecular docking output shows that the lowest binding energy for 2INP is -7.54 kcal/mol and most docked inhibitors interacted with the ligand within the 4HOE binding site.

REFERENCES

[1] T.C. Barden, Indoles: Industrial, Agricultural and Over-the-Counter Uses, Top Heterocycl Chem 26 (2011) 31–46.

[2] O.A. Luzina, D.N. Sokolov, M.A. Pokrovskii, A.G. Pokrovskii, O. B. Bekker, V.N. Danilenko N.F. Salakhutdinov, synthesis and biological activity of usnic acid Enamine derivatives, Chemistry of Natural Compounds, 51 (2015) 646-651.

[3] A.S. Salman, N.A. Mahmoud, A. Abdel-Aziem, M.A. Mohamed, D.M. Elsisi, synthesis, reactions and antimicrobial activity of some new 3-substituted indole derivatives, International Journal of Organic Chemistry, 5 (2015) 81-99.

[4] GaussView, Version 5, Roy Dennington, Todd Keith, and John Millam, *Semichem Inc.*, Shawnee Mission, KS, 2009.

[5] M. J. Frisch, G. W. Trucks, H. B. Schlegel, G. E. Scuseria, M. A. Robb, Gaussian 09, Revision **E.01,** Gaussian, Inc., Wallingford CT, 2009.

[6] A.M. Asiri, M. Akkurt, S. A. Khan, I. Ullah Khan and M.N. Arshad, "(E)-2-Cyano-3-[4-(dimethylamino)phenyl]- N -phenylprop-2-enamide", Acta Cryst. (2009). E65, o1303.

[7] N. Swarnalatha, S.Gunasekaran, S. Muthu, M. Nagarajan, Molecular structure analysis and spectroscopic characterization of 9-methoxy-2H-furo[3,2-g]chromen-2-one with experimental (FT-IR and FT-Raman) techniques and quantum chemical calculations, spectrochim. Acta part A 137 (2015) 721-729.

[8] L.G. Wade (Ed), Advanced Organic Chemistry, 4th ed., Wiley, New York,1992. p.723.

[9] N. Sundaraganesan, S.Illakiamani, C. Meganathan, B.D. Joshua, Vibrational spectroscopy investigation using ab initio and density functional theory analysis on the structure of 3-aminobenzotrifluoride, Spectrochim. Acta A 67 (2007) 214-224.

[10] Y.X. Sun, Q.L. Hao, W. X. Wei, Z. X. YU, D.D. LU. X. Wang, Y. S. Wang, Experimental and density functional studies on 4-(3,4-dihydroxybenzylideneamino)antipyrine, and 4-(2,3,4-trihydroxybenzylideneamino)antipyrine, J. Mol. Struct. Theochem. 904 (2009) 74-82.

[11] M. Nakano, H. Fujita, M. Takcathata, K. Yamaguchi, Theoretical Study on Second Hyperpolarizabilities of Phenylacetylene Dendrimer: Toward an Understanding of Structure−Property Relation in NLO Responses of Fractal

Antenna Dendrimers, J. Am. Chem. Soc. 124 (2002) 9648-9655.

[12] N.T. Abdel-Ghani , M.F.A. El-Ghar, A.M. Mansour, Novel Ni(II) and Zn(II) complexes coordinated by 2-arylaminomethyl-1H-benzimidazole: Molecular structures, spectral, DFT studies and evaluation of biological activity, Spectrochimica Acta A 104 (2013) 134-142.

[13] A.R. Katritzky, L. Mu, V.S. Lobanov, M. Karelson, Correlation of Boiling Points with Molecular Structure. 1. A Training Set of 298 Diverse Organics and a Test Set of 9 Simple Inorganics, J. Phys. Chem. 100 (1996) 10400-10407.